Bayesian inference of the magnetic component of quark-gluon plasma

Authors: *Yu Guo (郭钰), Jinfeng Liao (廖劲峰), and Shuzhe Shi (施舒哲)*

arXiv:2510.16838v1

Department of Physics - Tsinghua University

Guilin - 2025/10/26

The 16th Workshop on QCD Phase Transition and Relativistic Heavy-Ion Physics (QPT 2025)

QCD matter and the confinement problem

color confinement

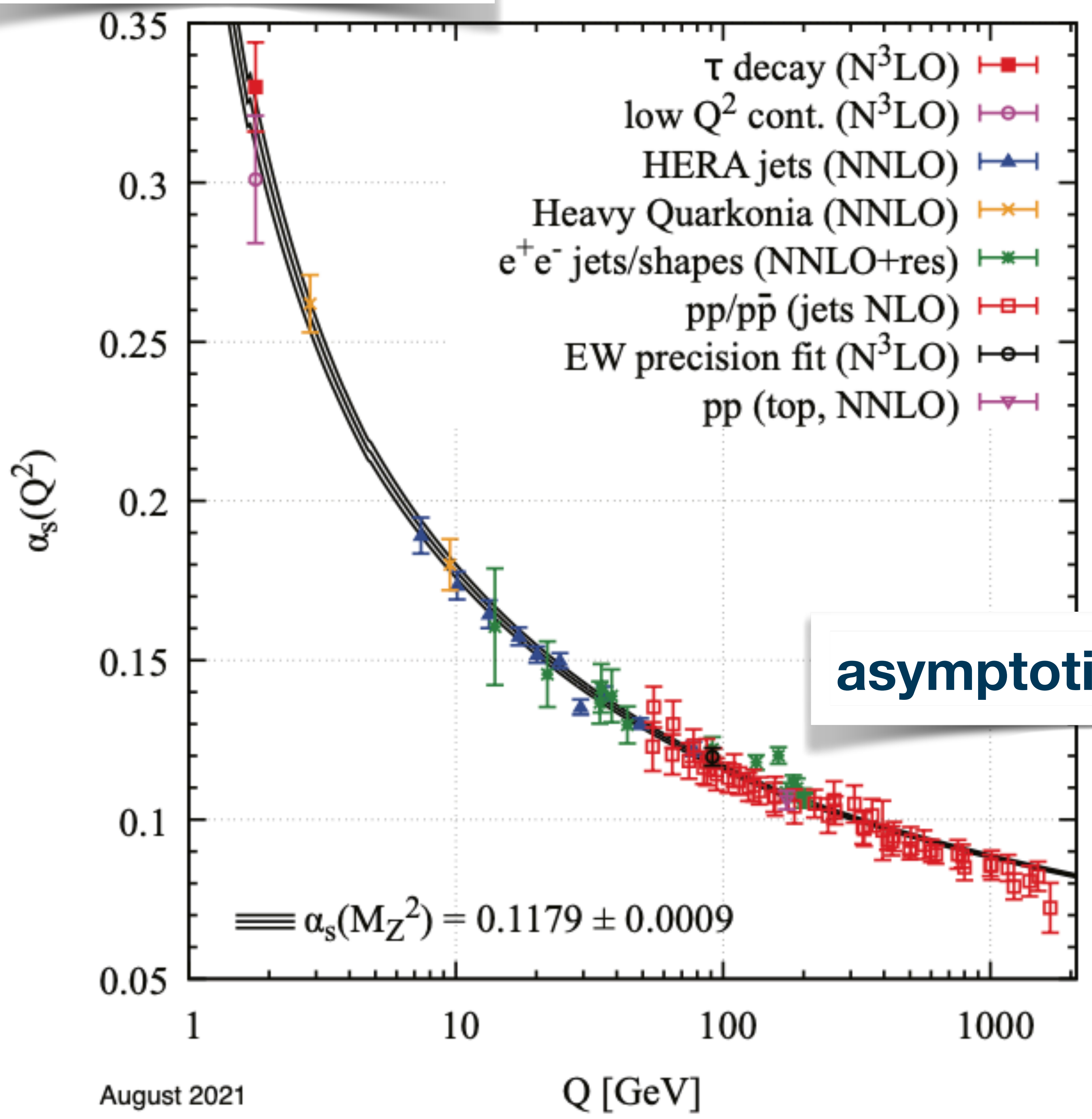

asymptotic freedom

[PDG Group - PTEP 2022, 083C01 (2022)]

crossover

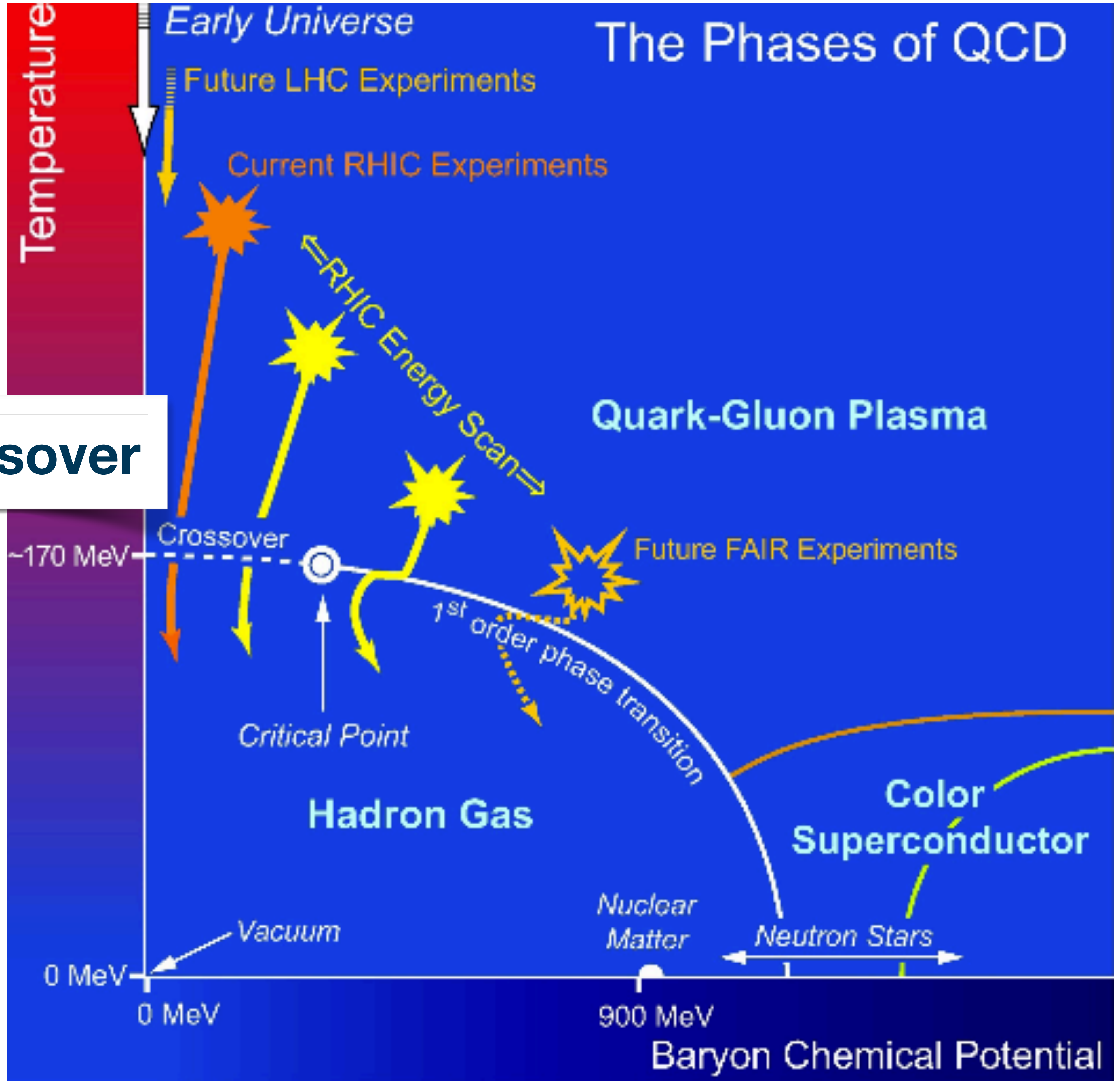

[https://www.bnl.gov/newsroom/news.php?a=21870]

Jet quenching

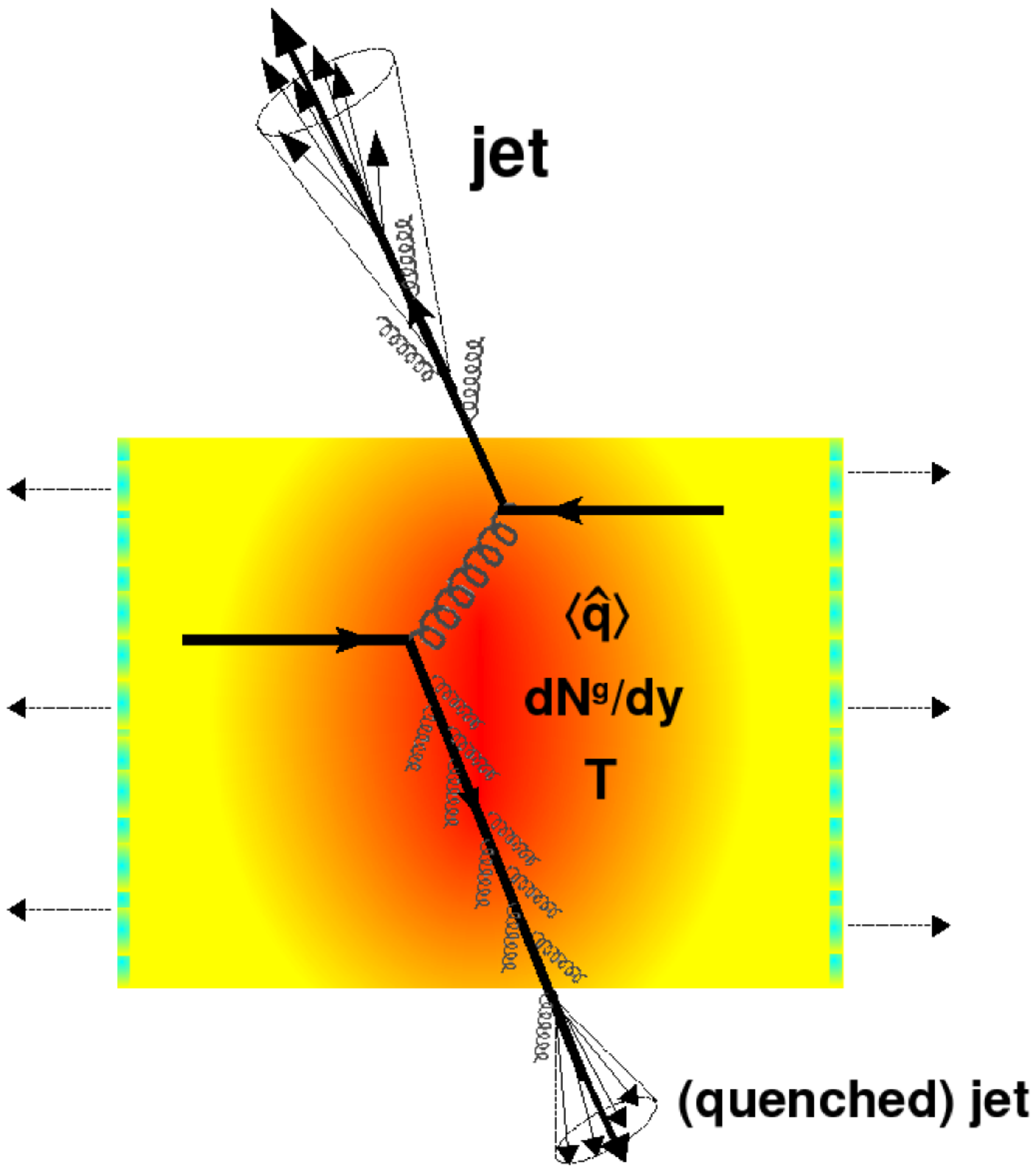

[Landolt-Bornstein 23 (2010) 471]

High-p_T partons produced in initial hard scatterings.

Carrying information of jet–medium interactions:

- Elastic scattering
- Inelastic (radiative) energy loss

Fragment into hadrons.

The nuclear modification factor:

$$R_{AA}(p_T, y) = \frac{1}{\langle T_{AA} \rangle} \frac{d^2N_{AA}/dp_T\,dy}{d^2\sigma_{pp}/dp_T\,dy}$$

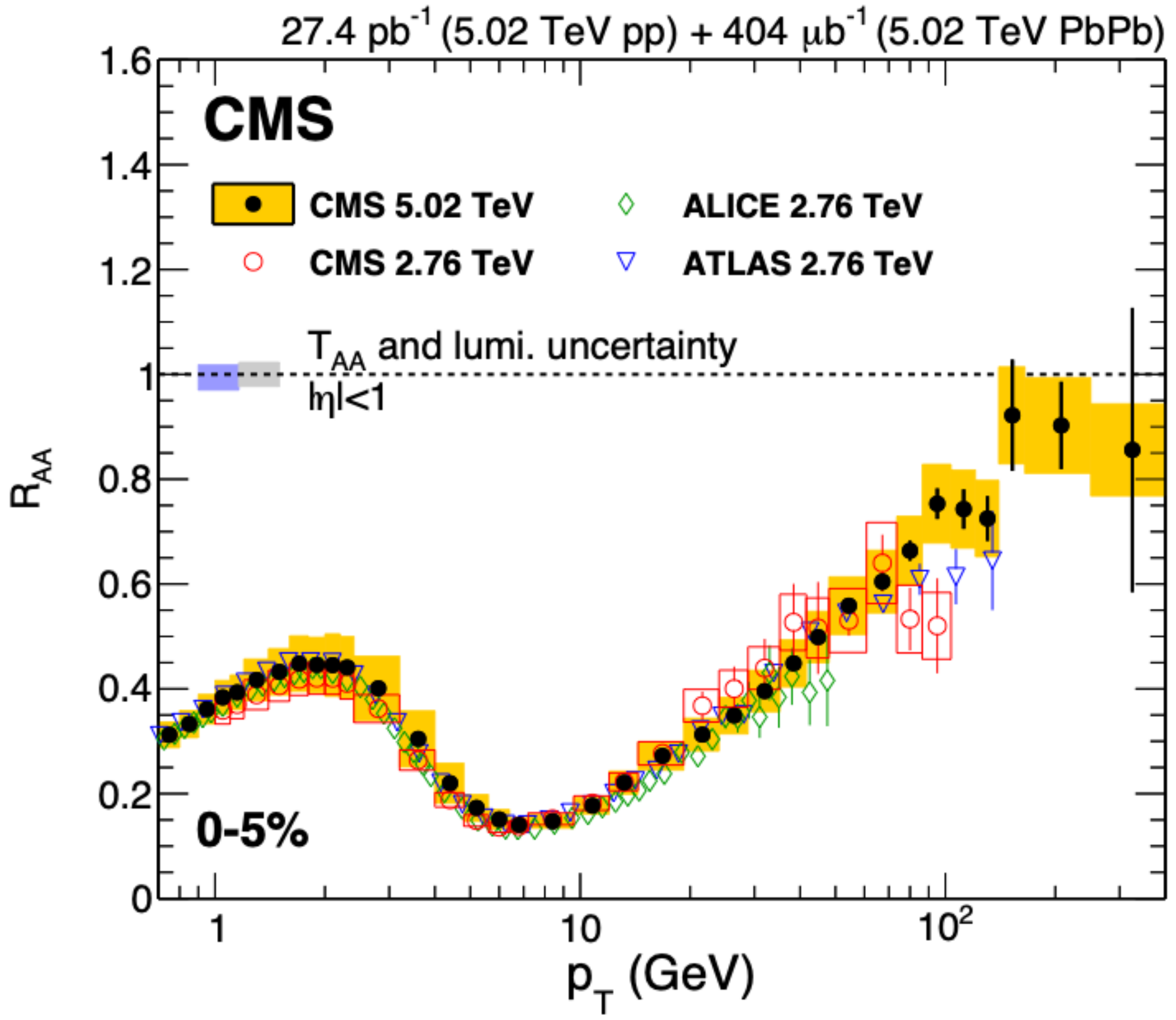

[CMS - JHEP04(2017)039]

$R_{AA} \otimes v_2$ puzzle

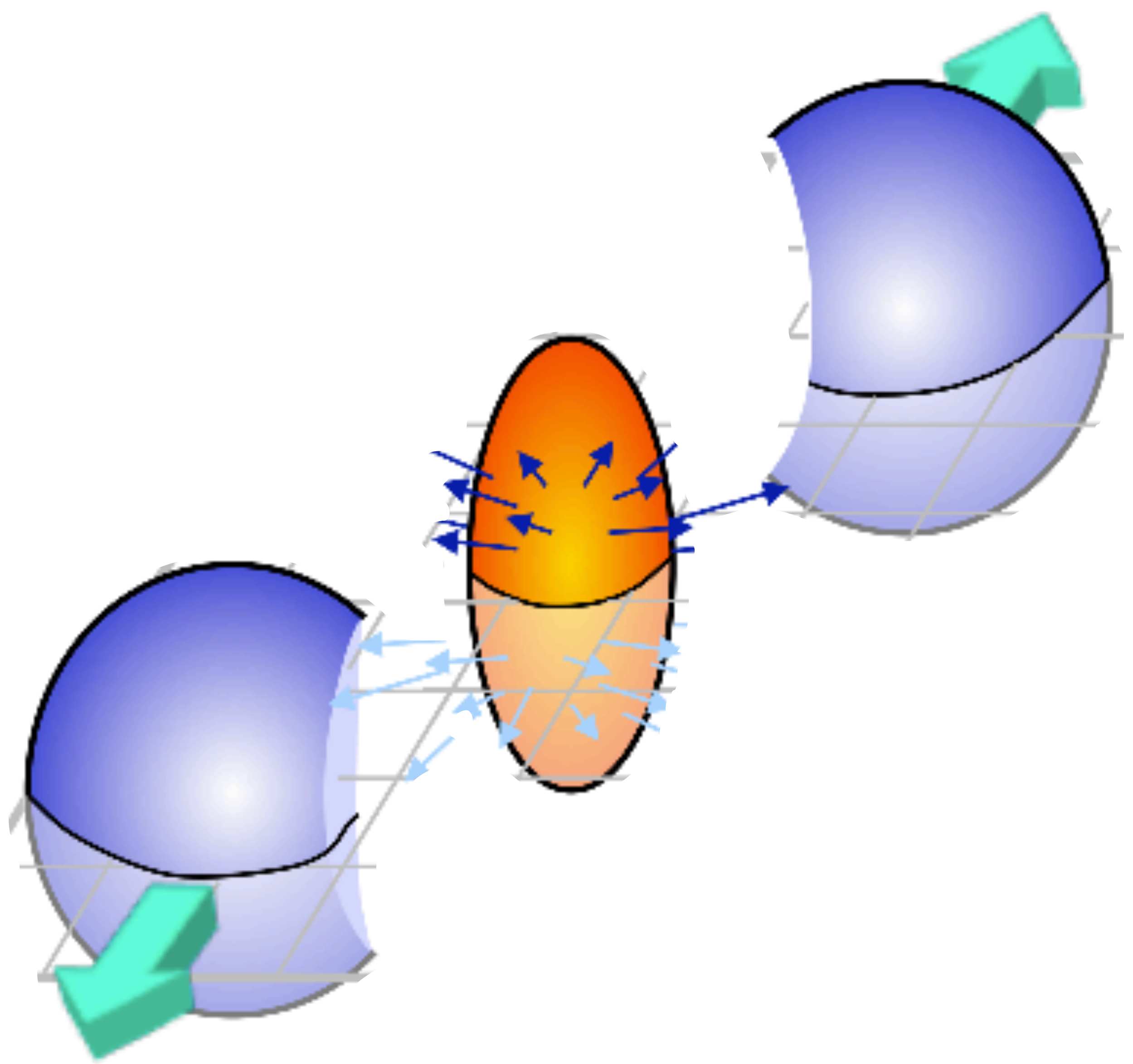

[Phys. Scripta T 158, 014004 (2013)]

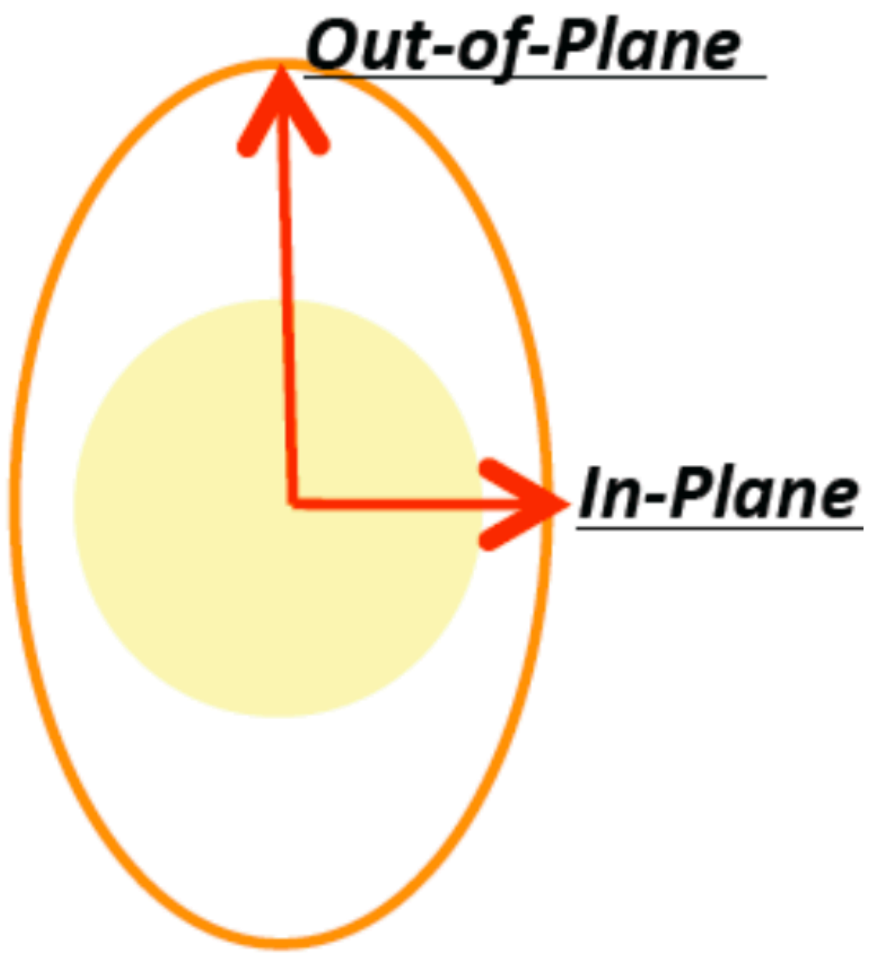

$\hat{q}(T) \propto T^3$

[JHEP08(2014)063]

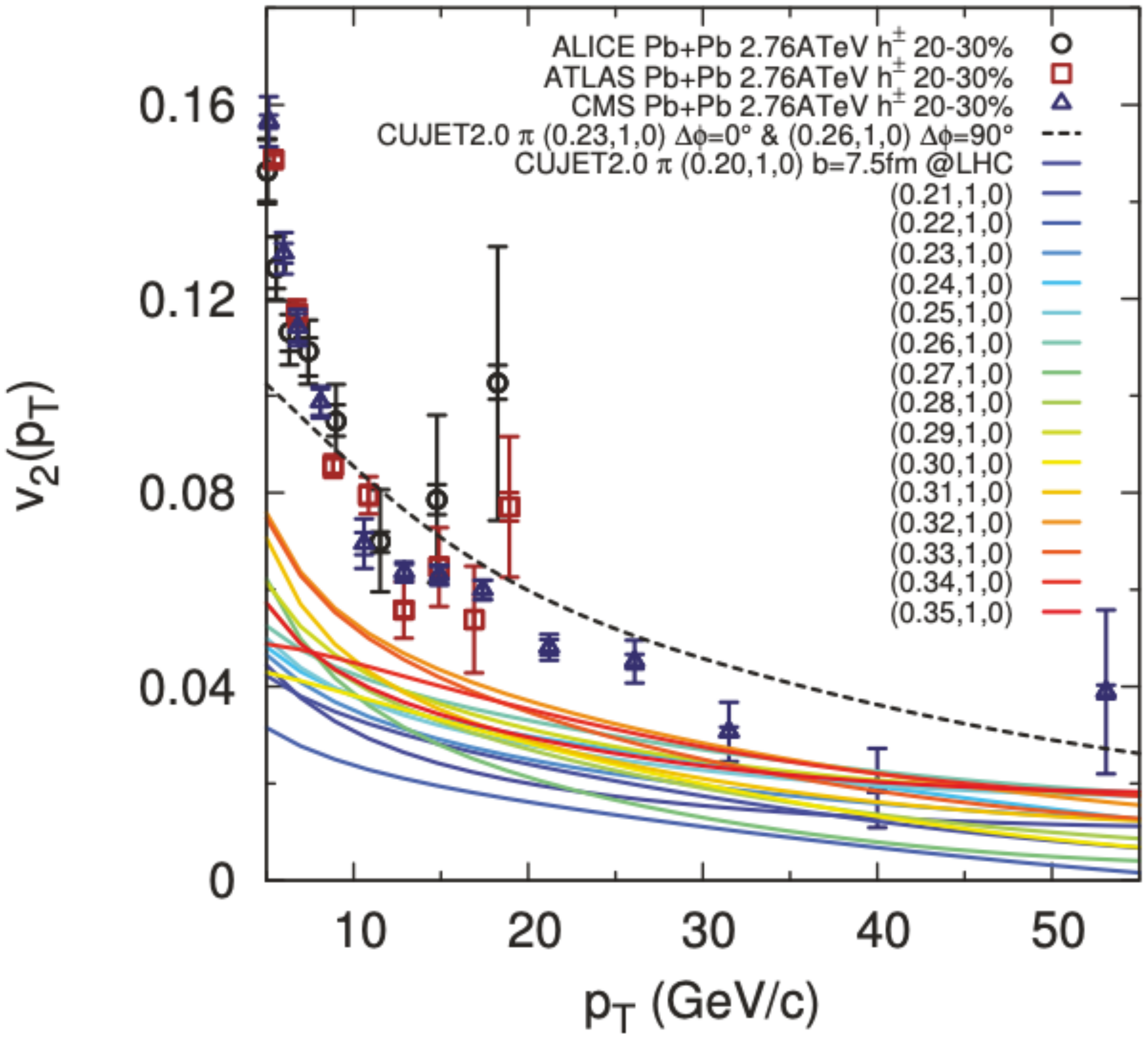

$v_2(p_T \gtrsim 8-10\ \mathrm{GeV/c})$ → jet-quenching anisotropy

or path-length dependent v_2

$$v_2^{\text{high } p_T} \simeq \frac{R_{AA}^{\text{in}} - R_{AA}^{\text{out}}}{R_{AA}^{\text{in}} + R_{AA}^{\text{out}}}$$

Tuning to R_{AA} usually underestimates v_2 ——

A long-standing $R_{AA} \otimes v_2$ tension.

From puzzle back to the confinement problem

Possible missing DoF near T_c:

chromo-magnetic monopoles

PHYSICAL REVIEW C **75**, 054907 (2007)

Strongly coupled plasma with electric and magnetic charges

Jinfeng Liao and Edward Shuryak

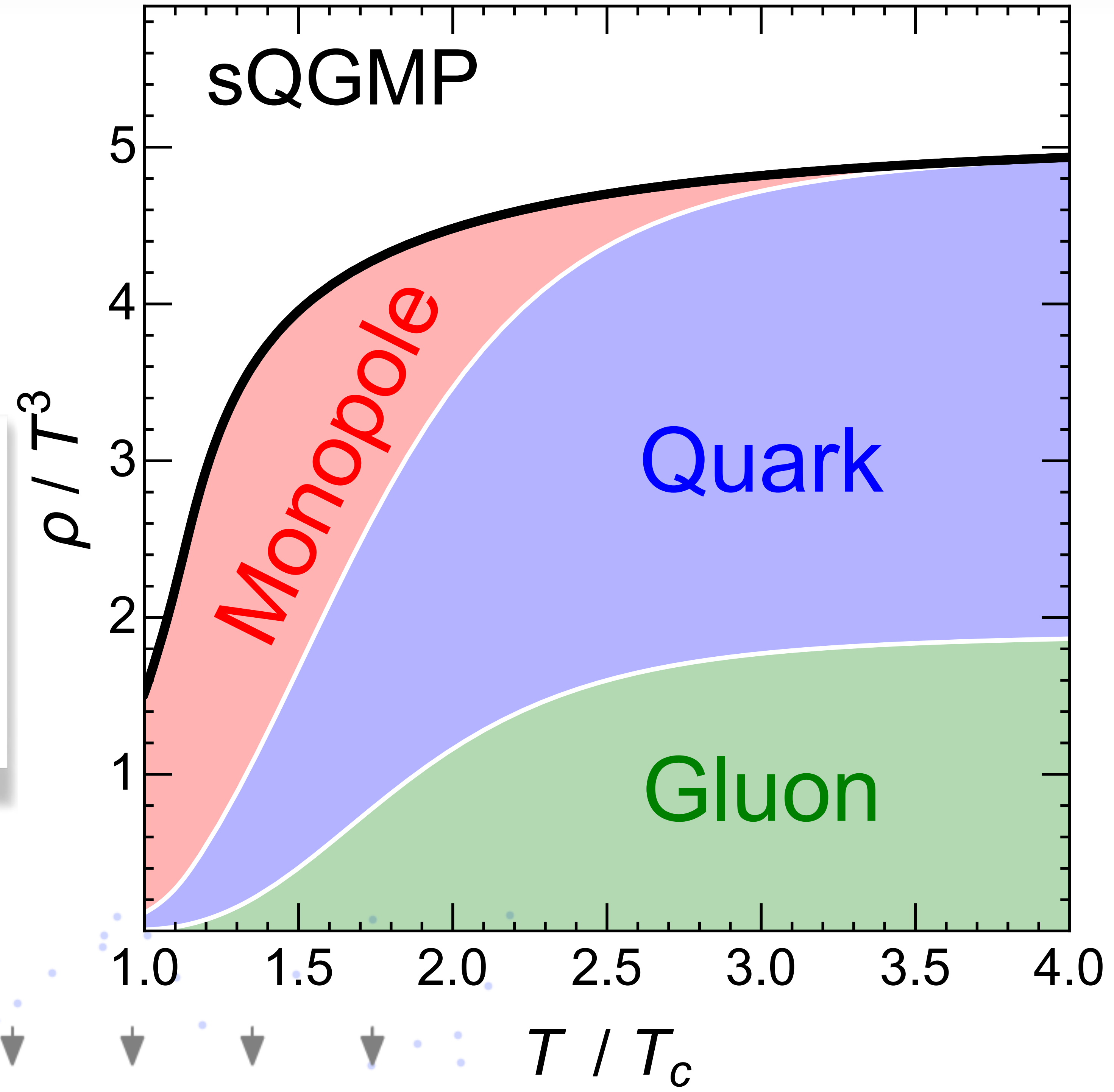

Dirac quantization:

$$\alpha_E\ \alpha_M = 1$$

weak electric

strong magnetic coupling near T_c

enhances jet–medium interaction

larger v_2

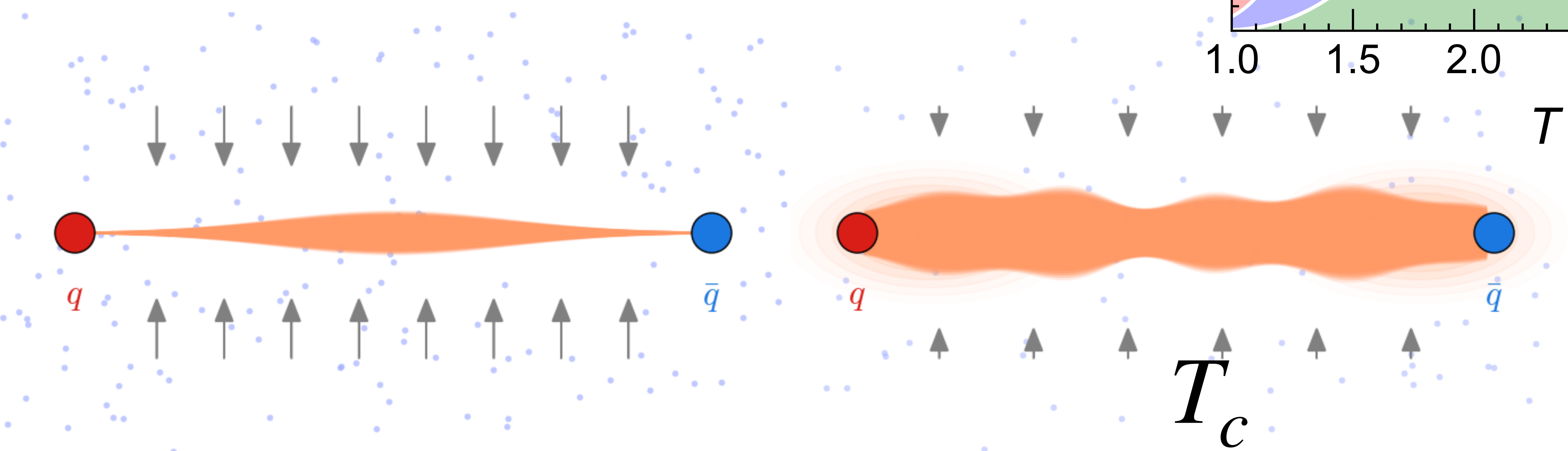

T_c $\sim 3T_c$

strongly coupled confined phase

strongly coupled QGP

asymptotically free QGP

CUJET3 model

1. Hard scattering:

Generate high-p_T partons from pQCD pp spectra.

Bridging soft-hard transport properties of quark-gluon plasmas with CUJET3.0

[doi:10.1007/JHEP02(2016)169]

Jiechen Xu,[a] Jinfeng Liao[b,c] and Miklos Gyulassy[a]

2. Medium evolution:

Use (2+1)D viscous hydrodynamics (VISHNU) to provide $T(x, y, \tau)$.

3. Jet–medium interaction:

Sample local scattering centers

elastic + radiative energy loss via DGLV kernel.

$$\left[(3\rho_g + \frac{4}{3}\rho_q)\frac{\mathrm{d}\sigma_E}{\mathrm{d}\mathbf{q}_\perp^2} + 3\rho_m \frac{\mathrm{d}\sigma_M}{\mathrm{d}\mathbf{q}_\perp^2} \right]$$

4. Fragmentation:

Jets fragment into hadrons while($T < 160\,\mathrm{MeV}$ && out medium).

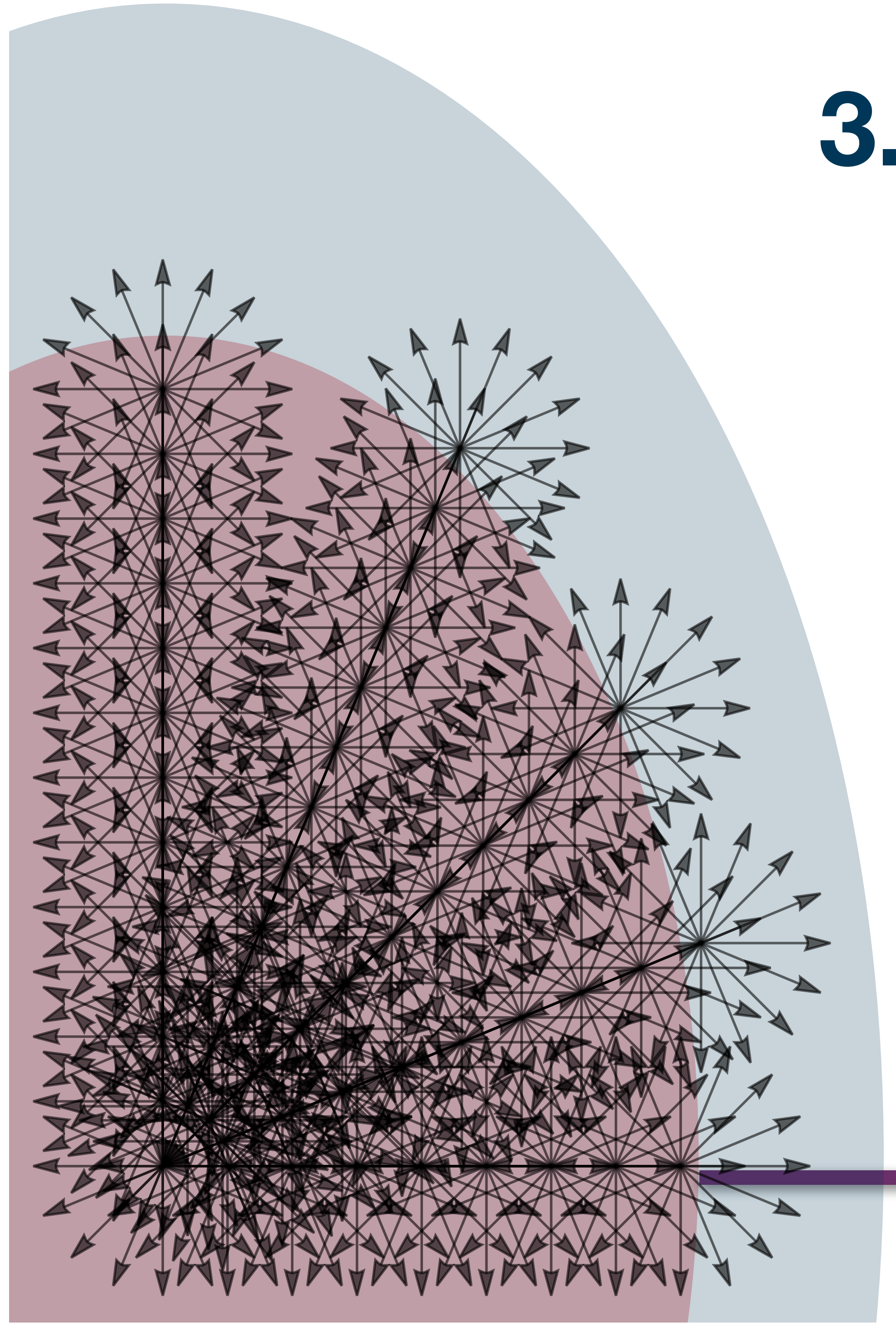

The DGLV-CUJET3 formalism

Gluon emission spectrum

$$x_E \frac{dN_g^{n=1}}{dx_E}$$

$$= \frac{3C_R}{\pi^2} \int d\tau \, \Gamma \int d^2\mathbf{k}_\perp \, \alpha_s\left(\frac{\mathbf{k}_\perp^2}{x_+(1-x_+)}\right)$$

$$\int d^2\mathbf{q}_\perp \left((3\rho_g + \frac{4}{3}\rho_q) \frac{\mathrm{d}\sigma_E}{\mathrm{d}\mathbf{q}_\perp^2} + 3\rho_m \frac{\mathrm{d}\sigma_M}{\mathrm{d}\mathbf{q}_\perp^2} \right)$$

$$\left(\frac{\mathbf{k}_\perp - \mathbf{q}_\perp}{(\mathbf{k}_\perp - \mathbf{q}_\perp)^2 + \chi^2} \cdot \left(\frac{\mathbf{k}_\perp - \mathbf{q}_\perp}{(\mathbf{k}_\perp - \mathbf{q}_\perp)^2 + \chi^2} - \frac{\mathbf{k}_\perp}{\mathbf{k}_\perp^2 + \chi^2} \right) \right)$$

$$\left(1 - \cos\left(\frac{(\mathbf{k}_\perp - \mathbf{q}_\perp)^2 + \chi^2}{2x_+ E} \tau \right) \right) \left| \frac{dx_+}{dx_E} \right|$$

$$\rho_g \equiv \chi_T \frac{16\,\rho}{16 + 9N_f}$$

$$\rho_q \equiv \chi_T \frac{9N_f\,\rho}{16 + 9N_f}$$

$$\rho_m = (1 - \chi_T)\rho$$

Diffenercial cross sections

$$\frac{\mathrm{d}\sigma_E}{\mathrm{d}\mathbf{q}_\perp^2} = \frac{f_E^2\,\alpha_s^2(\mathbf{q}_\perp^2)}{(\mathbf{q}_\perp^2 + f_E^2\mu^2)\,\mathbf{q}_\perp^2}, \quad \frac{\mathrm{d}\sigma_M}{\mathrm{d}\mathbf{q}_\perp^2} = \frac{f_M^2}{(\mathbf{q}_\perp^2 + f_M^2\mu^2)\,\mathbf{q}_\perp^2}$$

Screening factors

$$f_E = \sqrt{\chi_T(T)}, \quad f_M = c_M\sqrt{4\pi\alpha_s(\mu)}$$

Running coupling

$$\alpha_s(Q^2) = \frac{\alpha_C}{1 + \frac{9\alpha_C}{4\pi}\log(Q^2/\Lambda^2)}$$

Electrochromic/magnetic fractal

Past works estimated $\chi_T(T)$ via:

- Quark number susceptibility
- Polyakov loop

— — model assumptions.

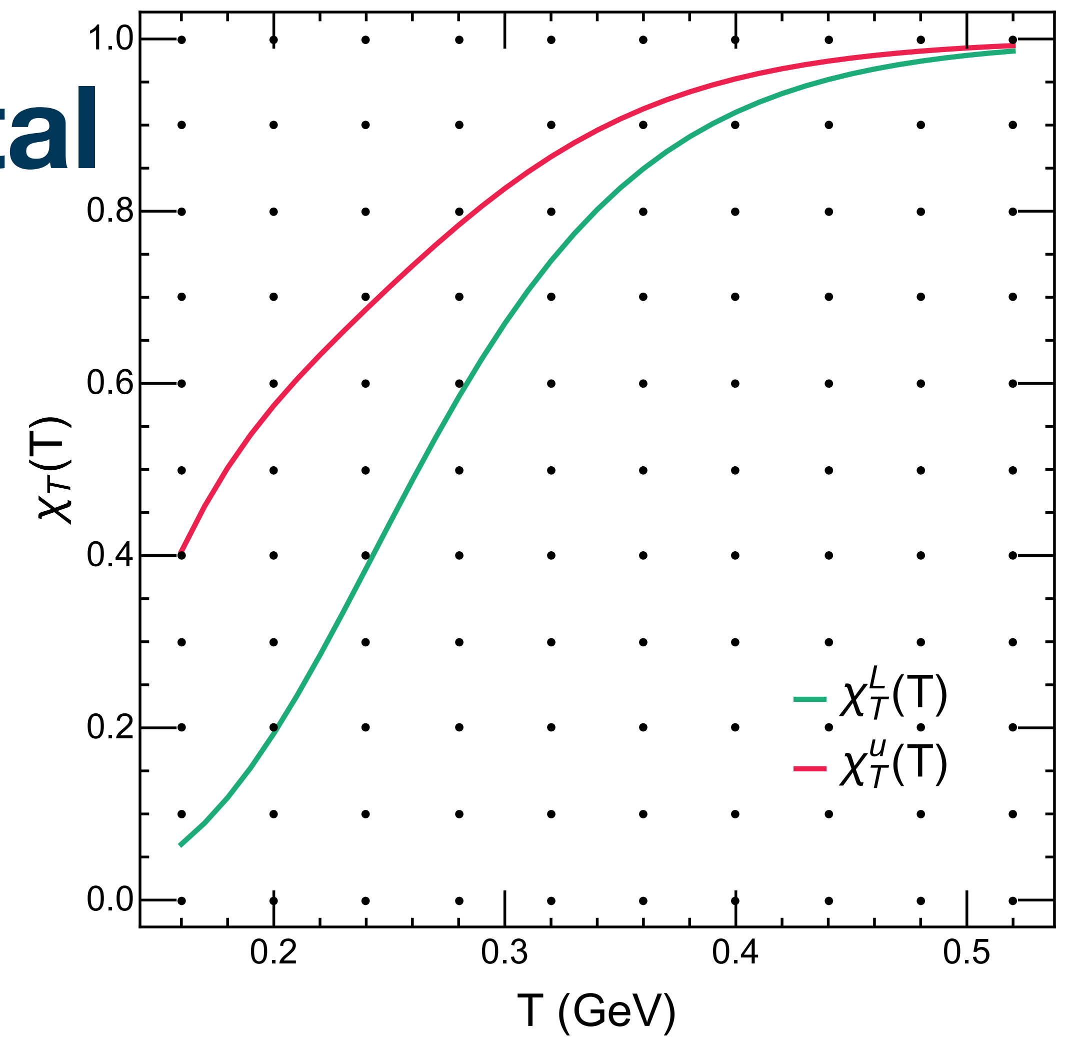

Here we constrain it directly from (R_{AA}, v_2).

Bayesian inference with explicit-likelihood (1/2)

Posterior distribution

$$p(\theta|\mathscr{D}) = \mathcal{N}_{\text{norm}}\, p(\mathscr{D}|\theta)\, p(\theta), \quad \boldsymbol{\theta} = \{\alpha_C, c_M, \chi_T(T_i)\}$$

Gaussian log-likelihood with diagonal covariance

$$\log p(\mathscr{D} \mid \theta) = -\frac{1}{2}\sum_{i=1}^{N}\left[\log(2\pi\sigma_i^2) + \frac{\left(\mathscr{D}_i - \hat{y}_i(\theta)\right)^2}{\sigma_i^2}\right]$$

Two prior

$\alpha_C \sim \text{Uniform}(0.3, 1.34)$

$c_M \sim \text{Uniform}(0.19, 0.56).$

$\chi_T(T)$ discretized at 10 temperature points in $[0.16,\ 0.52\ \text{GeV}]$:

1. Each $\chi_T(T_i)$ independent $\in [0,1]$.
2. $\chi_T(T)$ increases monotonically.

Experimental data

1. R_{AA}–v_2 pairs from the same collaborations.
2. Cover a broad range of energies, centralities and p_T.

Au+Au 200 GeV: 0–10%, 20–30%

PHENIX - Phys. Rev. C 87, 034911 (2013)
PHENIX - Phys. Rev. C 88, 064910 (2013)

Pb+Pb 2.76 TeV: 0–10%, 20–30%

ATLAS - JHEP 09, 050 (2015)
ATLAS - Phys. Lett. B 707, 330-348 (2012)

Pb+Pb 5.02 TeV: 0–5%

CMS - JHEP 04, 039 (2017)
CMS - Phys. Lett. B 776, 195-216 (2018)

Bayesian inference with explicit-likelihood (2/2)

12-D Scaffold

- 666 design points
- 84 test set

PCA + Surrogate model (GPE)

- 100 points -> 15 points
- $f(\mathbf{x}) \sim \mathcal{GP}\left(m(\mathbf{x}), k(\mathbf{x}, \mathbf{x}')\right)$
- $k(\mathbf{x}, \mathbf{x}') = \sigma_f^2 \exp\left[-\frac{1}{2}\sum_i \frac{(x_i - x_i')^2}{\ell_i^2}\right]$

Achieved < 4% relative error on test set.
[Neural Information Processing Systems (NeurIPS) (2018)]

Inference

Use No-U-Turn Sampler (NUTS) to explore the posterior distribution. [Journal of Machine Learning Research 15, 1593-1623 (2014)]

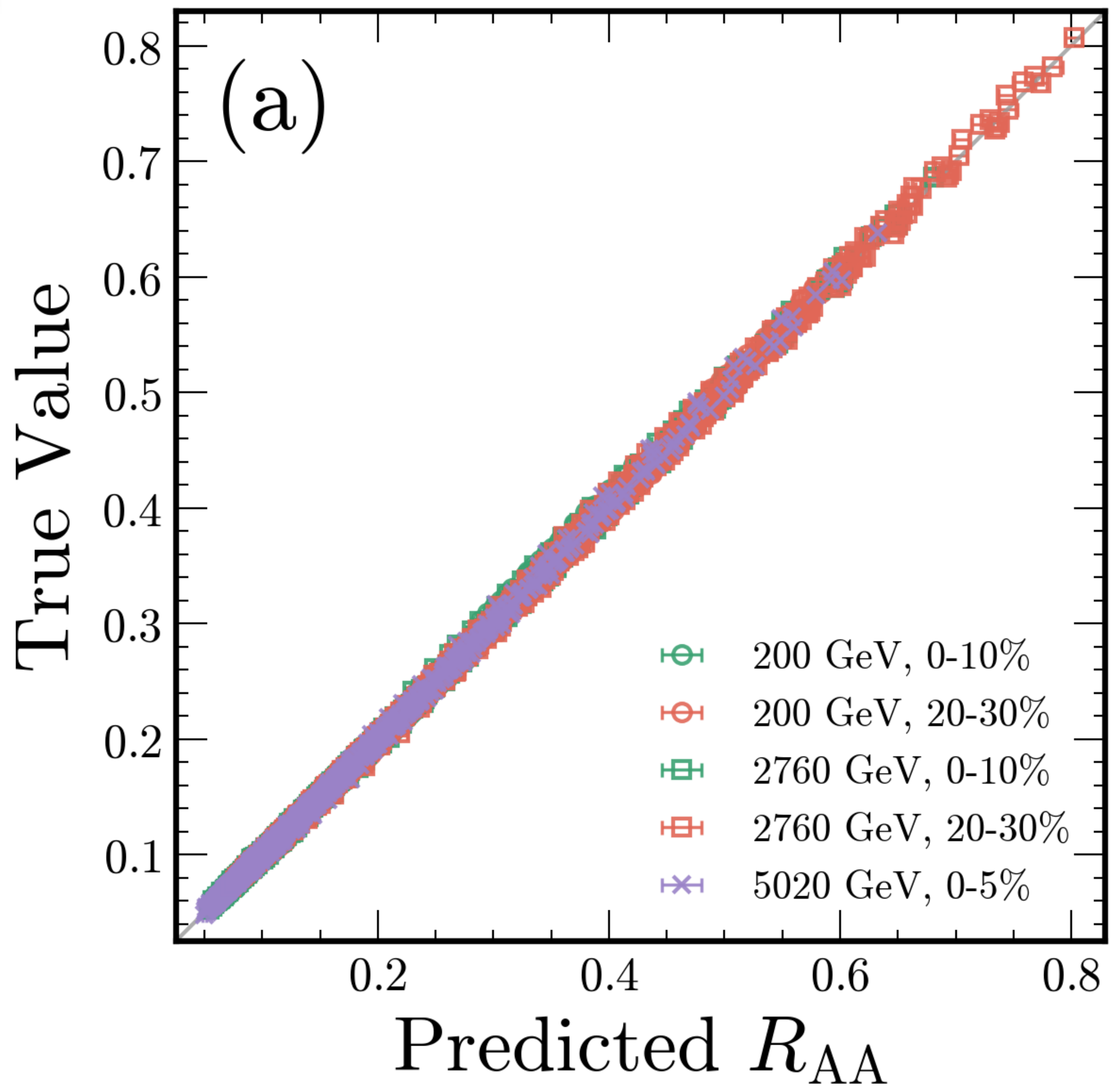

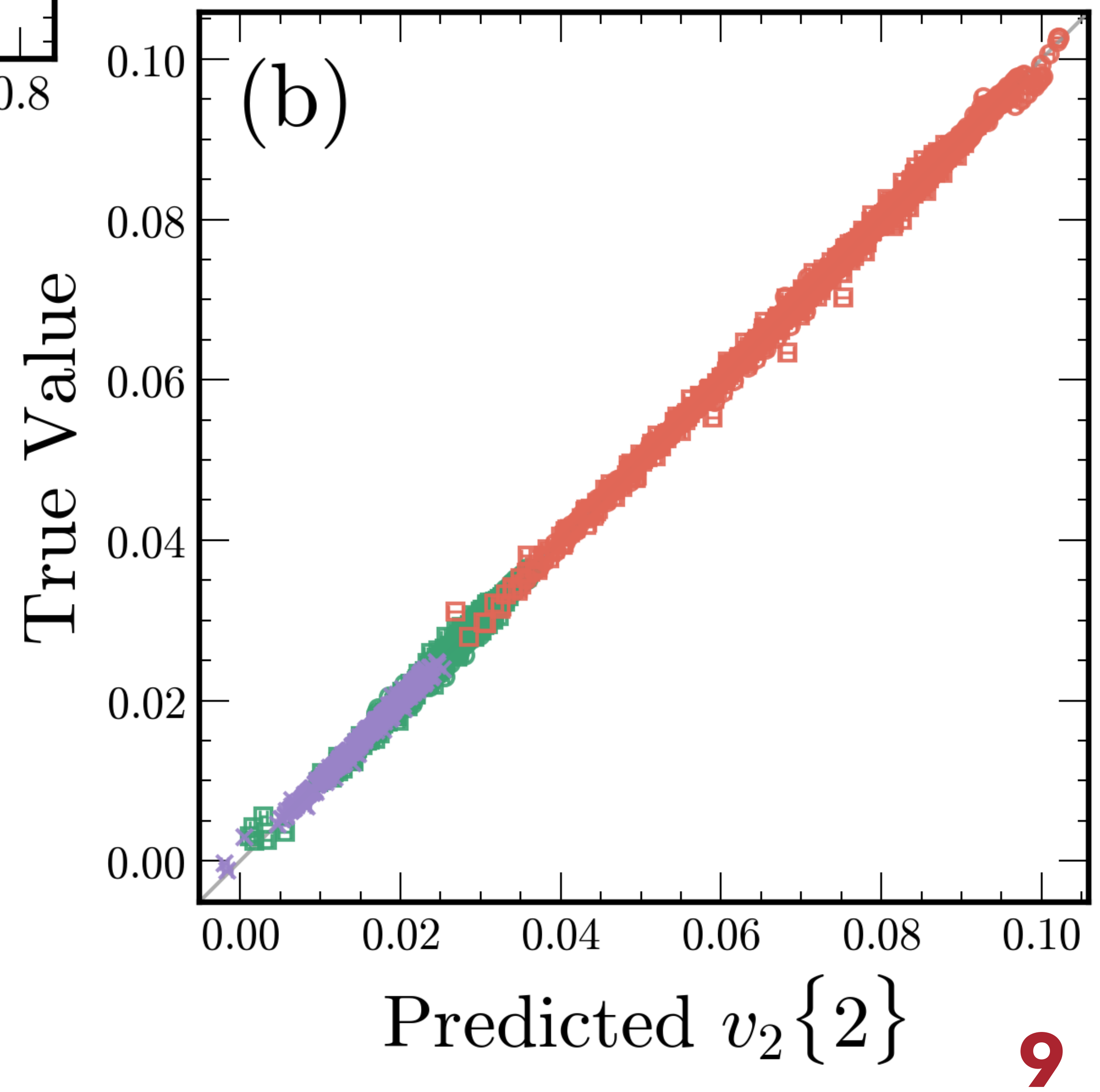

Design coverage

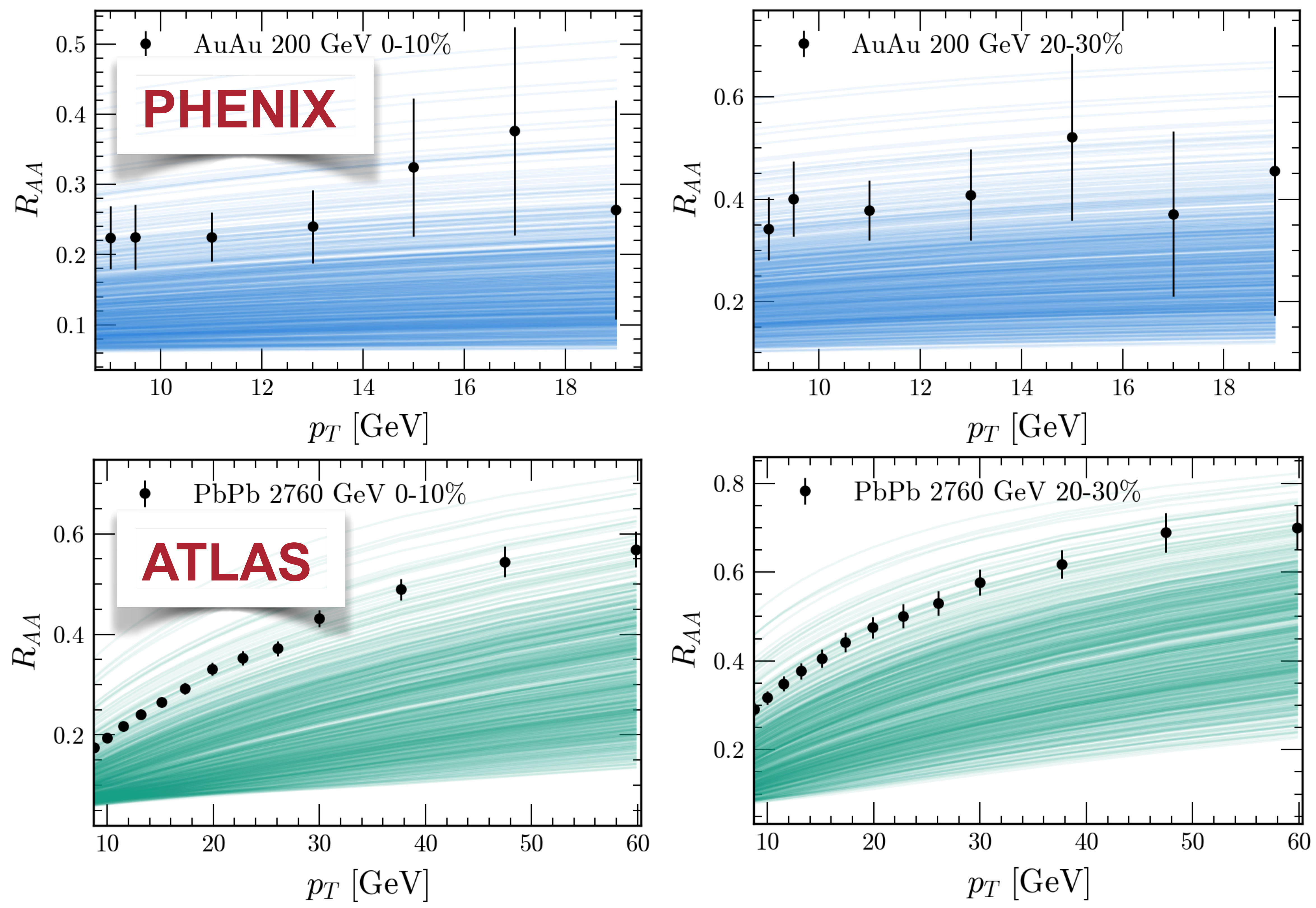

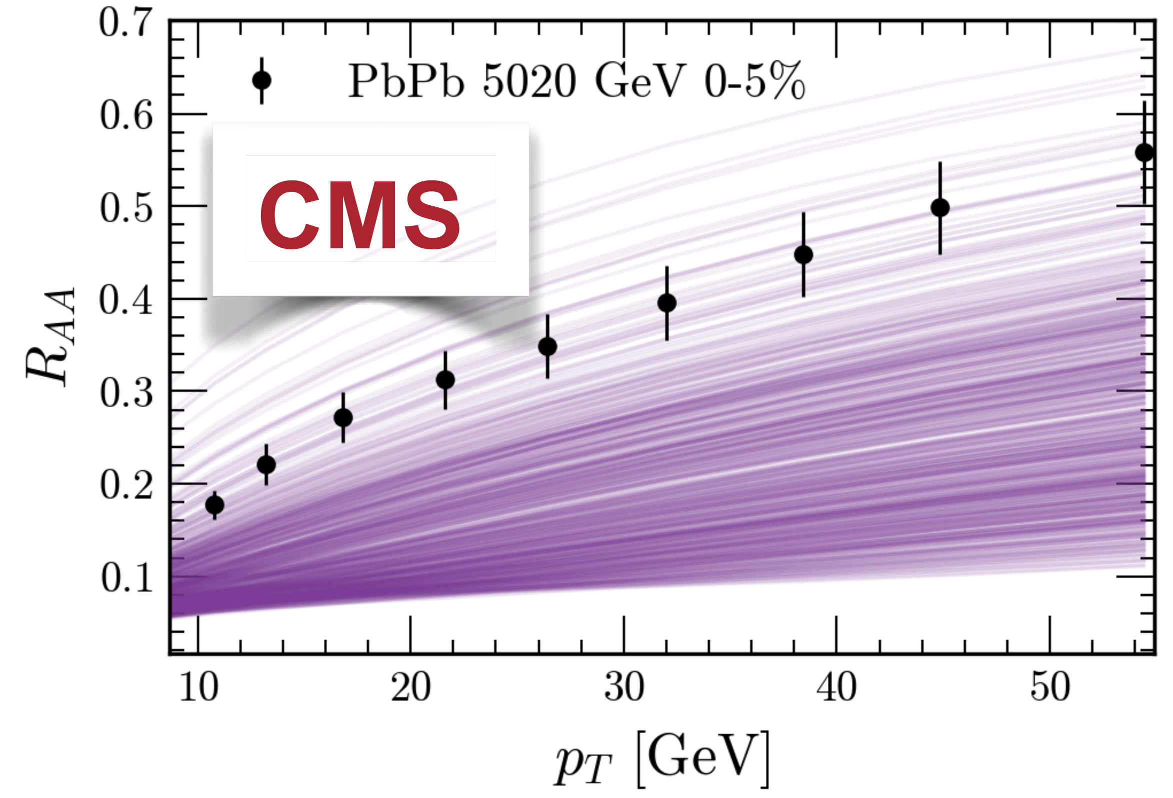

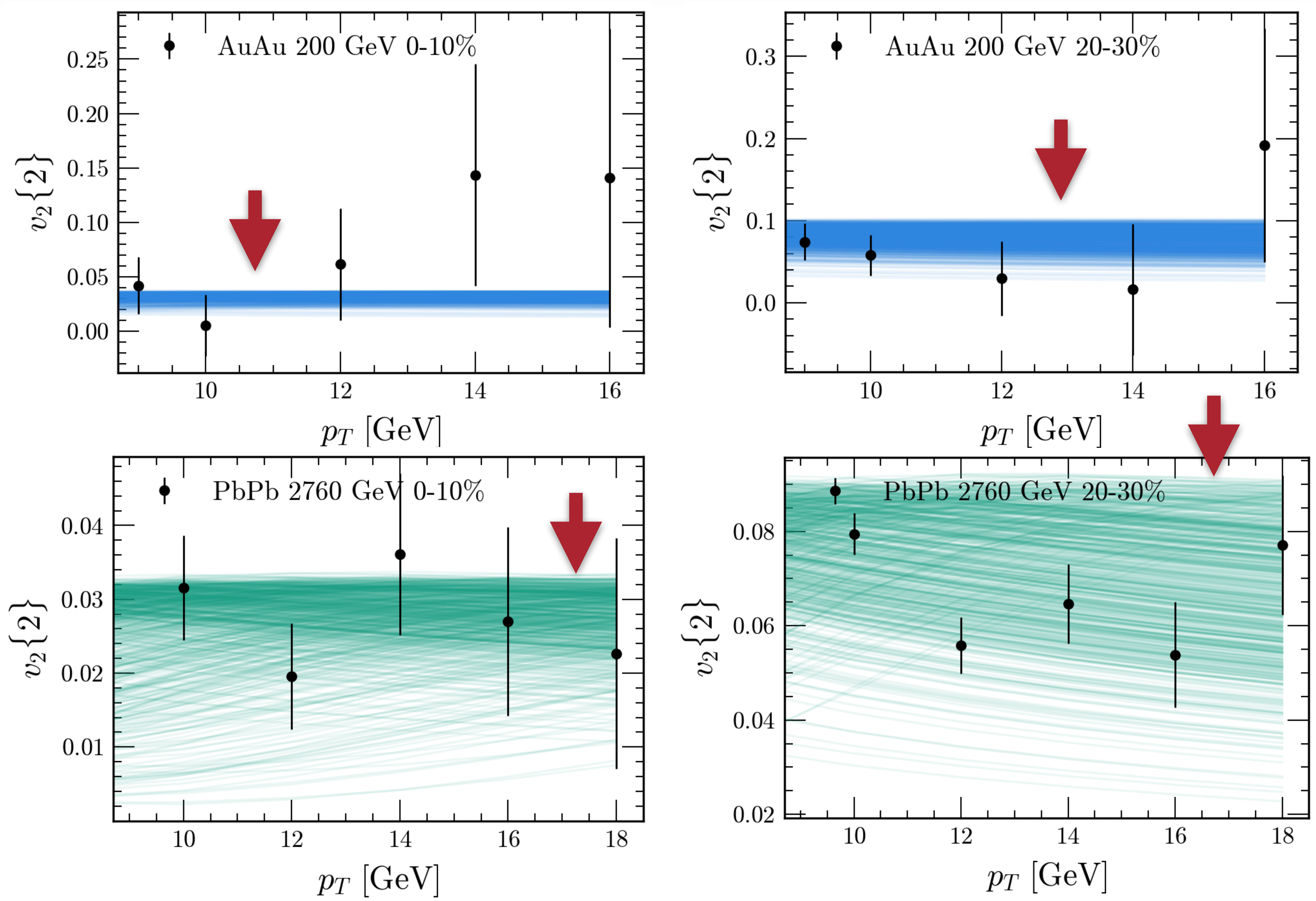

- The parameter space fully covers the physical range.
  - v_2 touch **the geometric limit** of path-length anisotropy.

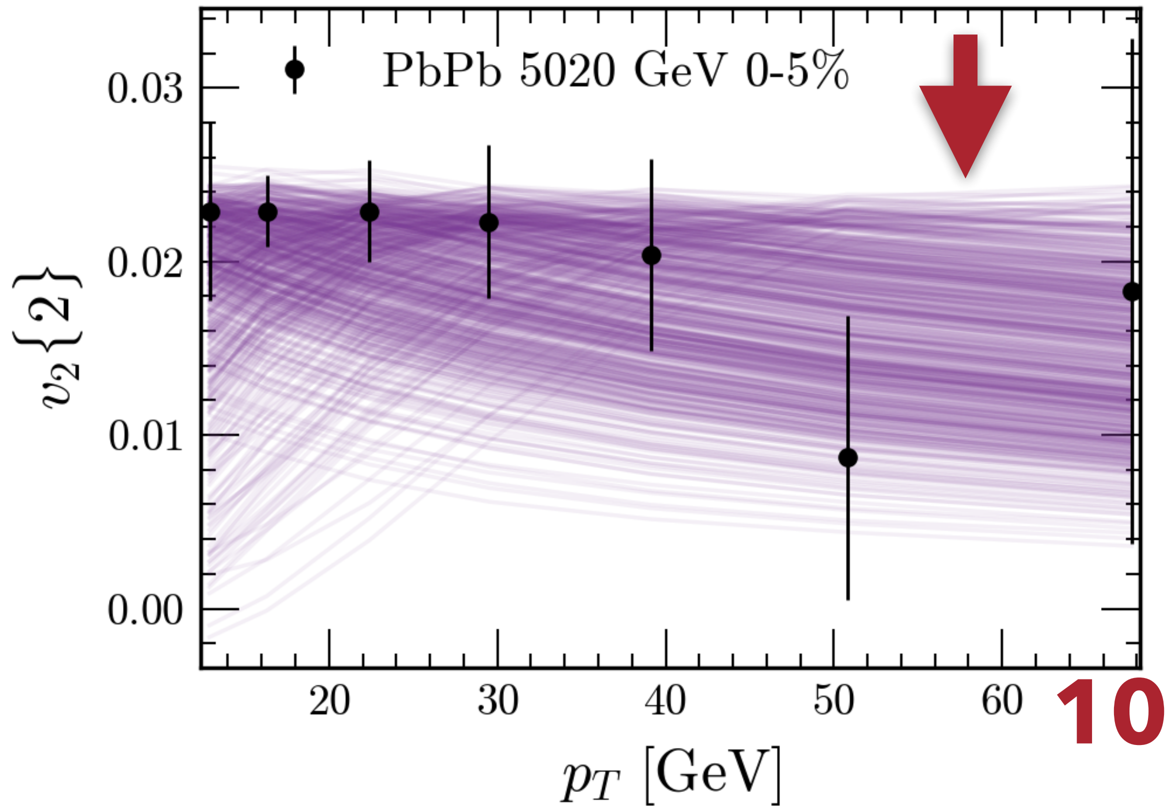

Calibration and predictions

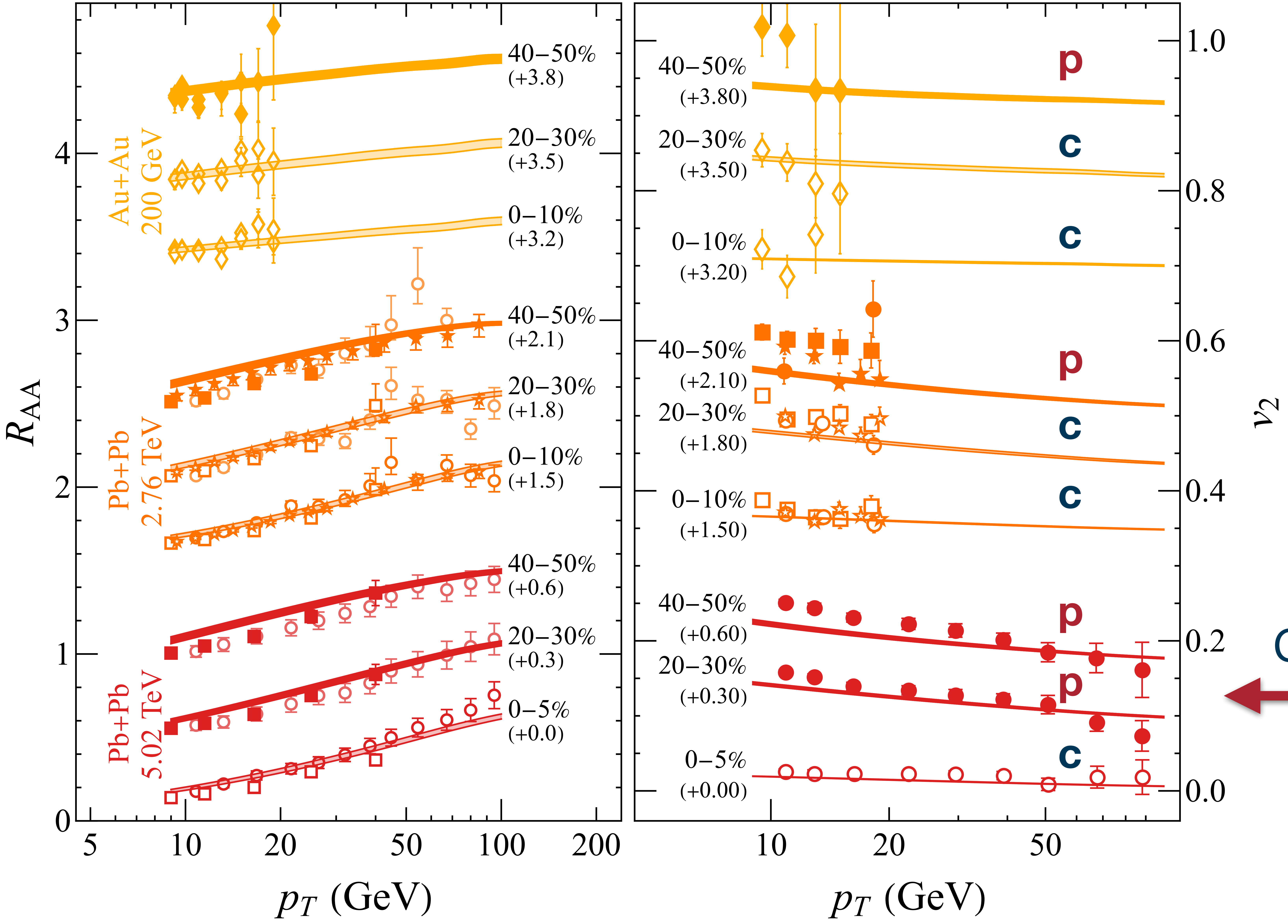

Additional data sets

Au+Au 200 GeV

PHENIX - Phys. Rev. Lett. 101, 232301 (2008)

Pb+Pb 2.76 TeV

ALICE - JHEP 11, 013 (2018)

ALICE - Phys. Lett. B 719, 18–28 (2013)

CMS - Eur. Phys. J. C 72, 1945 (2012)

CMS - Phys. Rev. C 87, 014902 (2013

Pb+Pb 5.02 TeV

ALICE - JHEP 11, 013 (2018)

CMS data 20-30% -> 10-30%

40-50% -> 30-50%

Posterior distribution

0.16

0.52

α_C

c_M

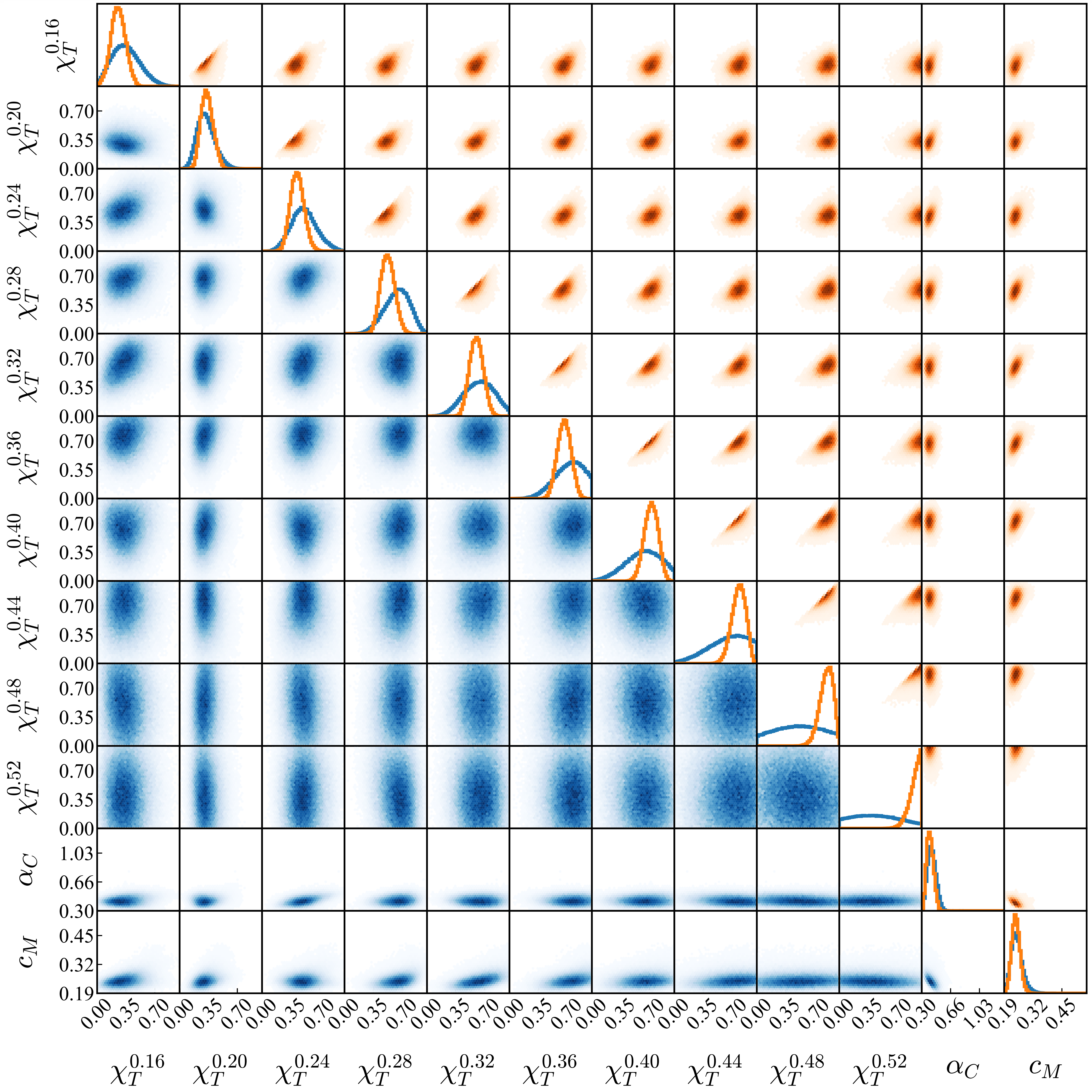

Median and $68~\%$ credible interval

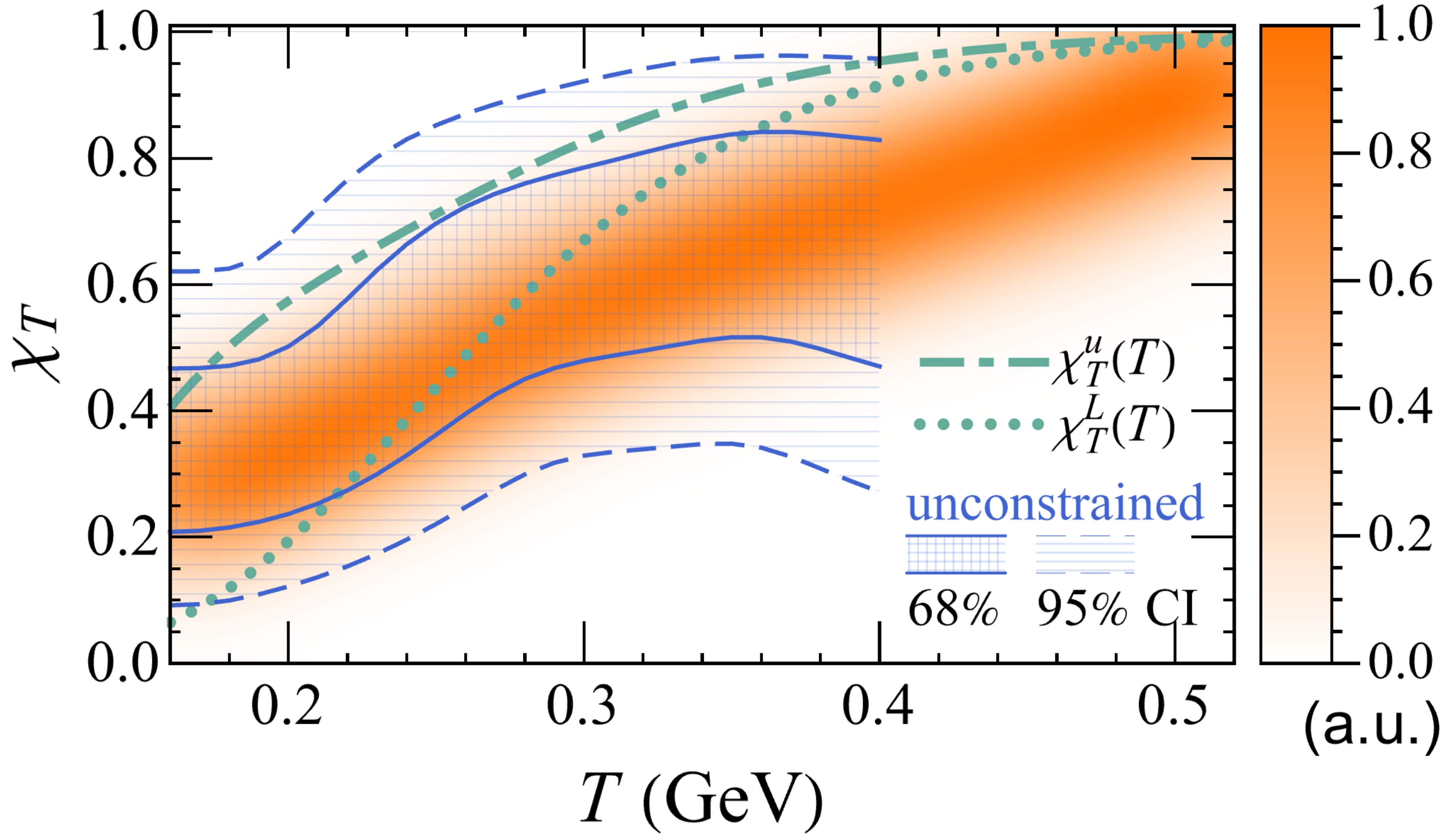

"unconstrained"

$$\alpha_C = 0.44^{+0.07}_{-0.06}, \quad c_M = 0.26^{+0.03}_{-0.03}$$

"monotonic"

$$\alpha_C = 0.43^{+0.05}_{-0.04}, \quad c_M = 0.25^{+0.02}_{-0.02}$$

Hard and soft transport coefficients

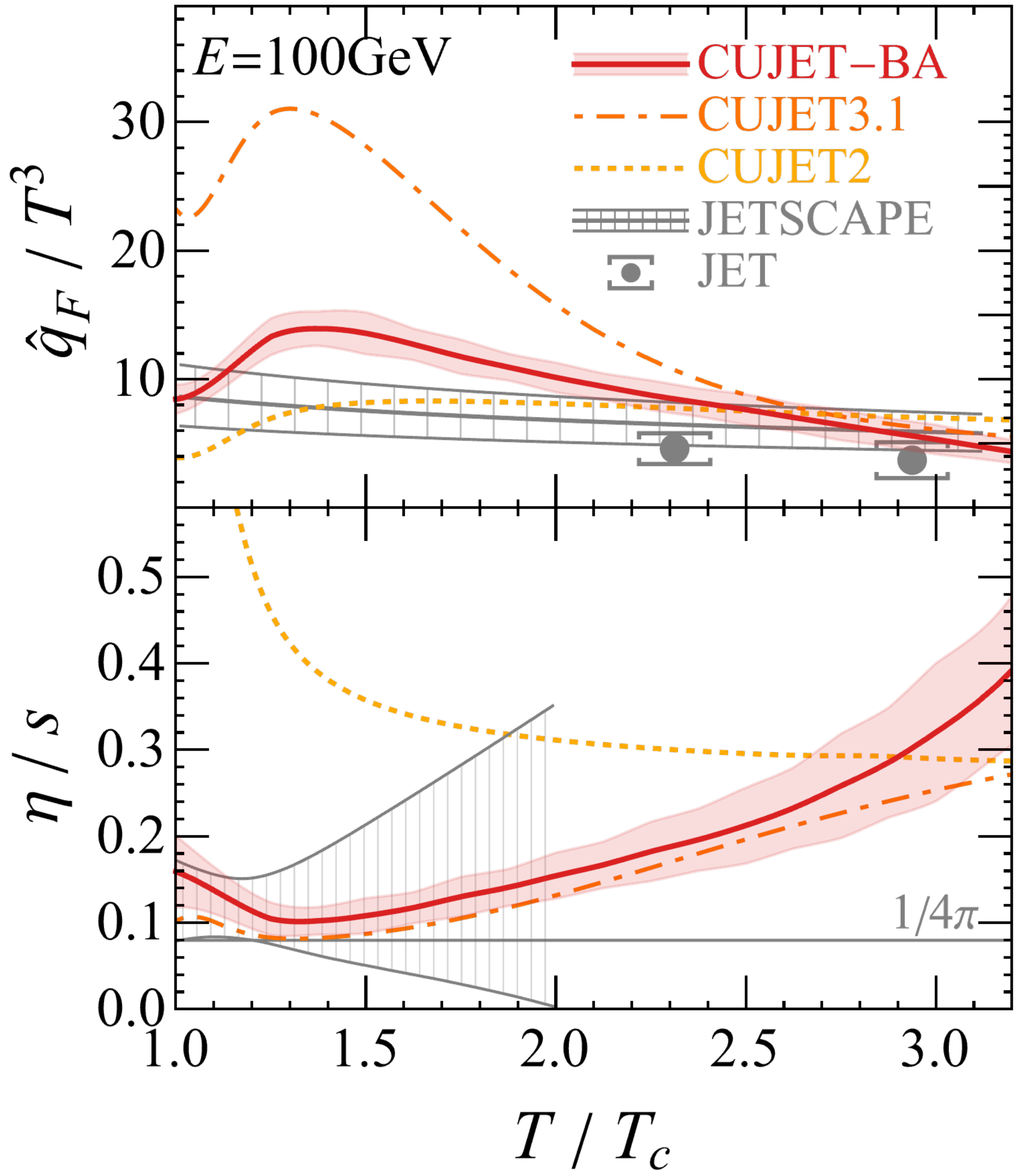

Jet transport coefficient

$$\hat{q}_a(E,T) = \int_0^{6ET} \mathbf{q}_\perp^2 d^2\mathbf{q}_\perp \sum_b C_{ab}\,\rho_b\,\alpha_s^{i_b}(\mathbf{q}_\perp^2)\frac{\mathrm{d}\sigma_b}{\mathrm{d}\mathbf{q}_\perp^2}$$

Shear-viscosity-to-entropy-density ratio

$$\frac{\eta}{s} = \frac{18T^3}{5s} \sum_{a\in\{g,q,m\}} \rho_a/\hat{q}_a\;(E = 3T/2)$$

Heavy quark diffusion coefficient

$$D_s = 4T^2/\hat{q}_F(E = 3\ \mathrm{GeV})$$

$$\hat{q}_F = \frac{C_F}{C_A}\hat{q}_a$$

Heavy-quark spatial diffusion coefficient

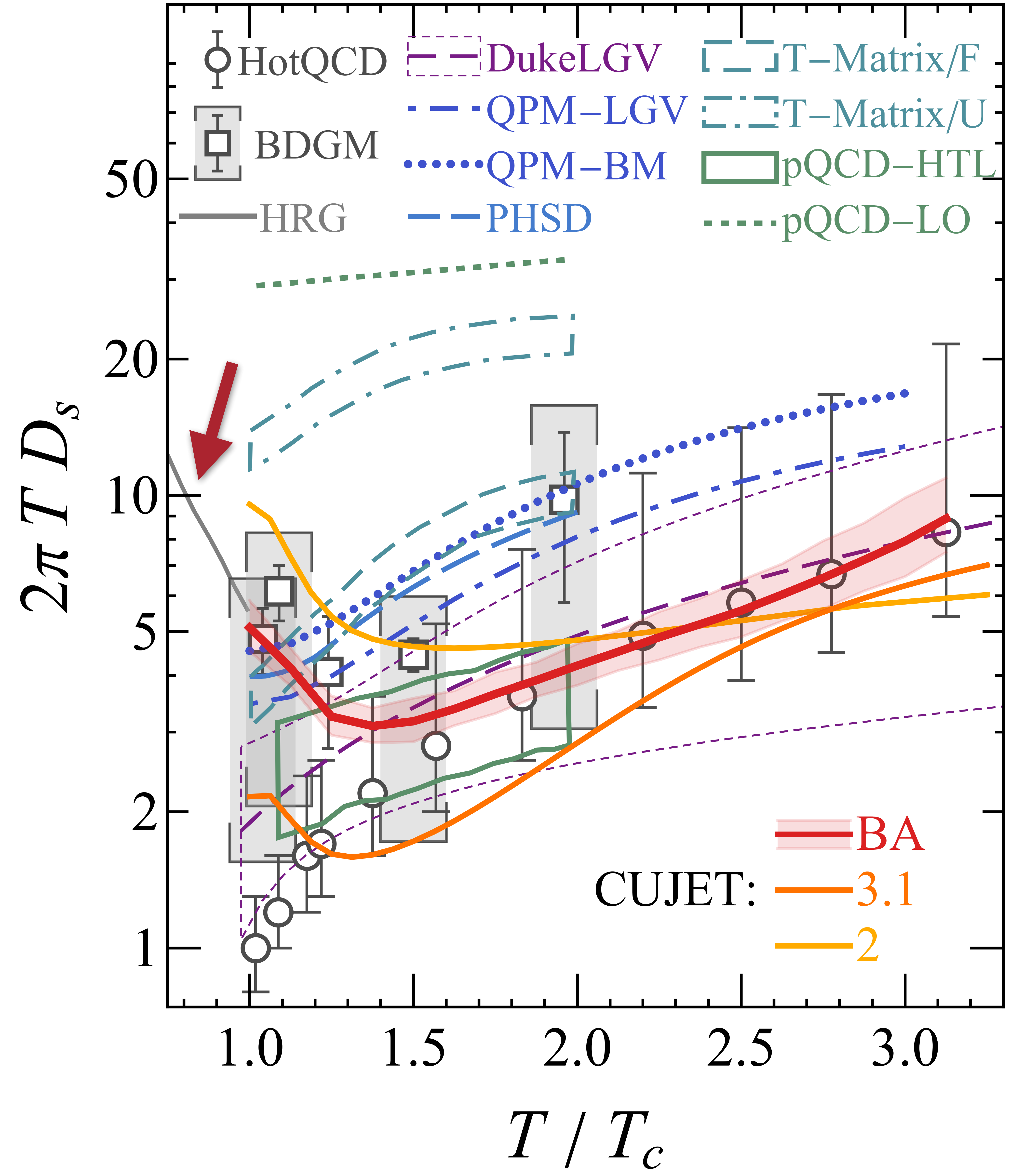

Jet transport coefficient

$$\hat{q}_a(E,T) = \int_0^{6ET} \mathbf{q}_\perp^2 d^2\mathbf{q}_\perp \sum_b C_{ab}\, \rho_b\, \alpha_s^{i_b}(\mathbf{q}_\perp^2) \frac{\mathrm{d}\sigma_b}{\mathrm{d}\mathbf{q}_\perp^2}$$

Shear-viscosity-to-entropy-density ratio

$$\frac{\eta}{s} = \frac{18T^3}{5s} \sum_{a\in\{g,q,m\}} \rho_a/\hat{q}_a\,(E=3T/2)$$

Heavy quark diffusion coefficient

$$D_s = 4T^2/\hat{q}_F(E = 3\ \mathrm{GeV})$$

$$\hat{q}_F = \frac{C_F}{C_A}\hat{q}_a$$

Summary

- Bayesian inference with CUJET3 reveals a strong magnetic component of QGP near T_c.
- Achieving simultaneous agreement with R_{AA} and v_2.
- Quantitatively reproducing key transport coefficients — $\hat{q}/T^3$, η/s, and D_s.

<u>This provides robust, data-driven evidence for emergent chromo-magnetic monopoles.</u>

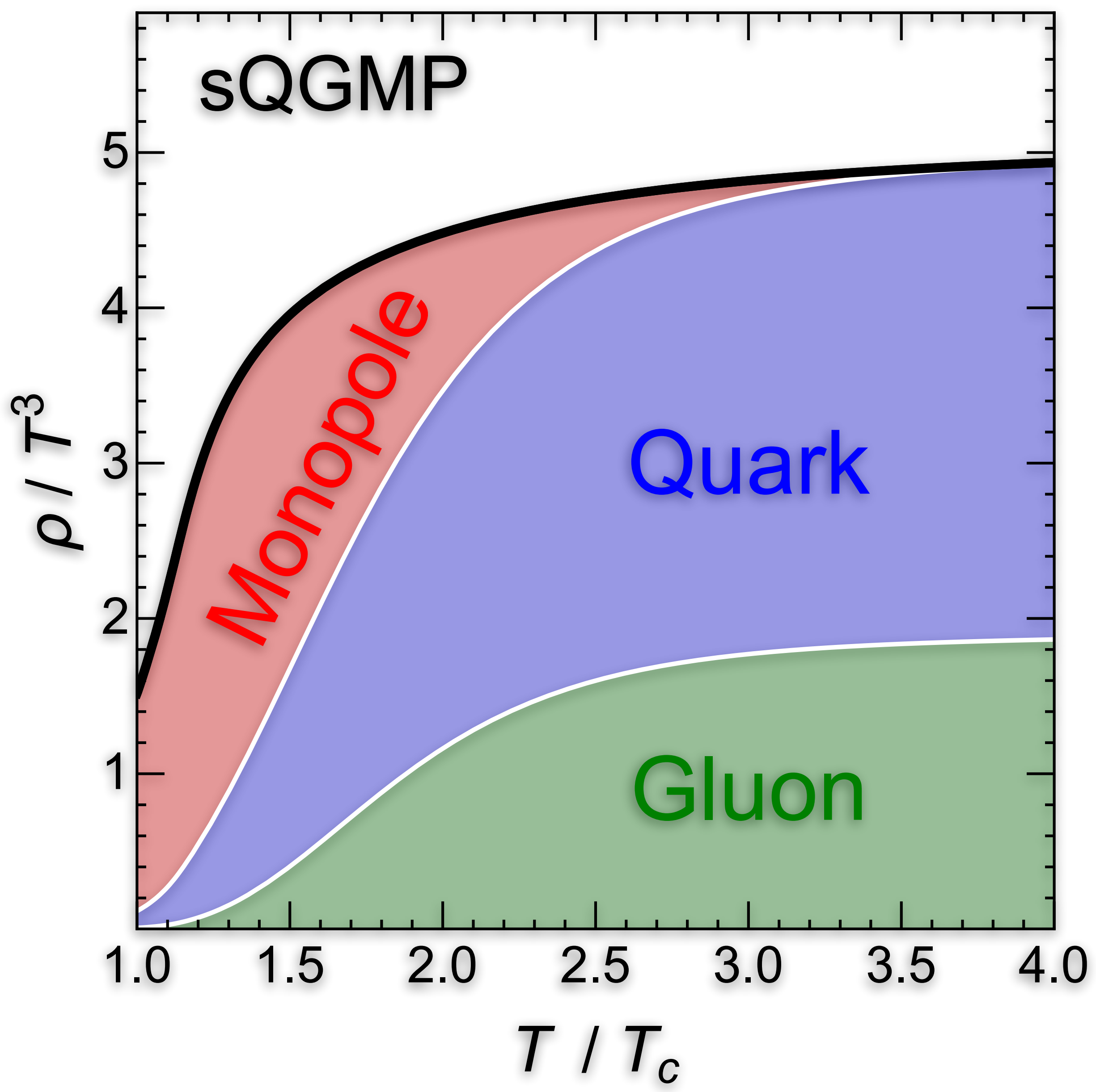

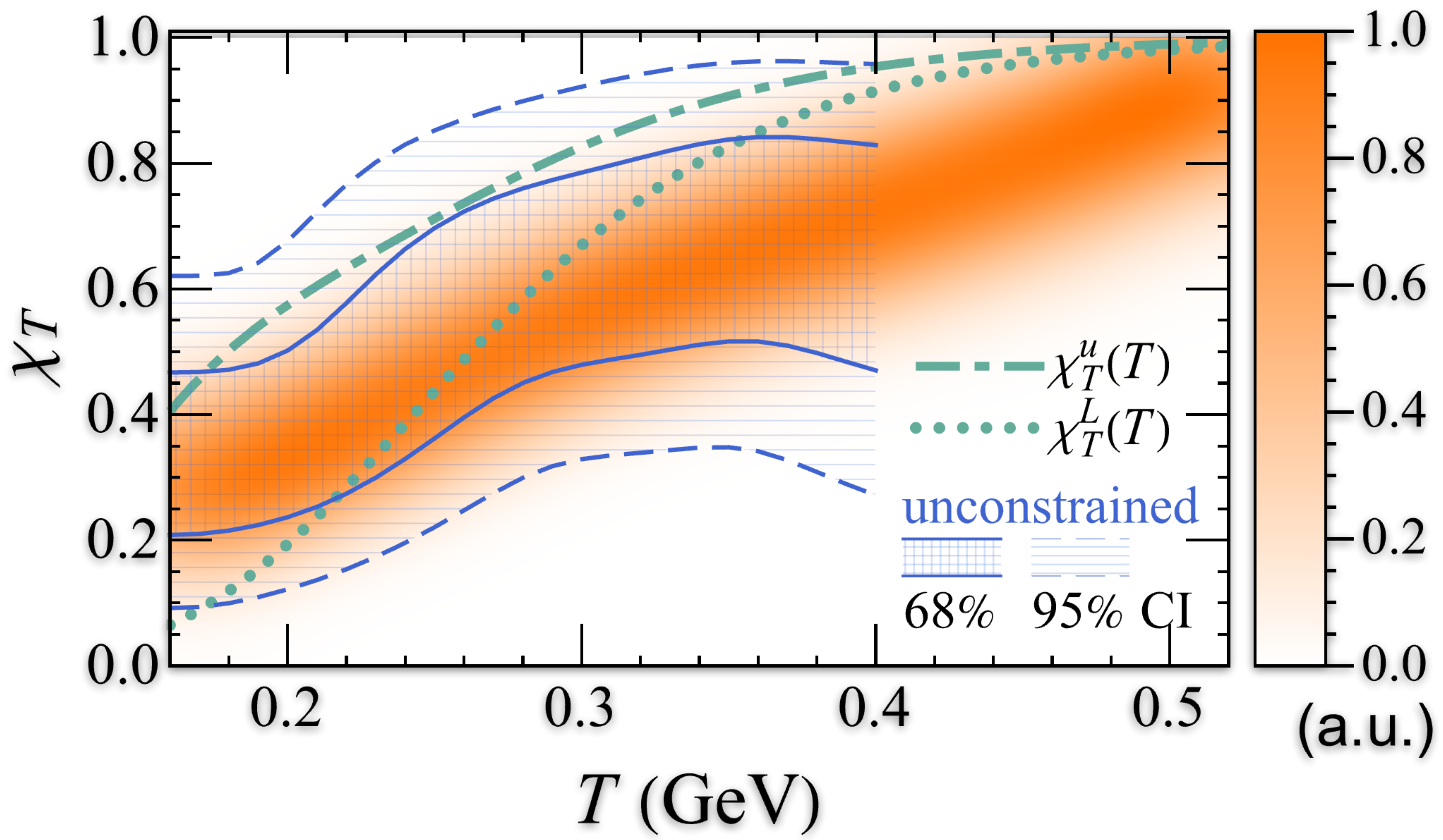

Thanks

About likelihood

Formally, consider two observables c_1, c_2 with residuals

$$r_i(\boldsymbol{\theta}) = c_{i,\text{model}}(\boldsymbol{\theta}) - c_{i,\text{obs}}, \quad i = 1, 2. \tag{6}$$

The true covariance matrix and the corresponding precision matrix of the experimental and emulator uncertainties can be expressed as

$$\Sigma_{\text{true}} = \begin{pmatrix} \sigma_1^2 & \rho\,\sigma_1\sigma_2 \\ \rho\,\sigma_1\sigma_2 & \sigma_2^2 \end{pmatrix}, \tag{7}$$

$$\Sigma_{\text{true}}^{-1} = \frac{1}{\sigma_1^2\sigma_2^2(1-\rho^2)} \begin{pmatrix} \sigma_2^2 & -\rho\,\sigma_1\sigma_2 \\ -\rho\,\sigma_1\sigma_2 & \sigma_1^2 \end{pmatrix}. \tag{8}$$

By substituting the precision matrix $\Sigma_{\text{true}}^{-1}$ into the logarithmic form of Eq. 3 and neglecting the additive normalization constant (which does not affect relative probabilities), the quadratic form in the log-likelihood reads

$$-2\log\mathcal{L}_{\text{true}} \propto \frac{1}{1-\rho^2}\left[\frac{r_1^2}{\sigma_1^2} - 2\rho\,\frac{r_1 r_2}{\sigma_1\sigma_2} + \frac{r_2^2}{\sigma_2^2}\right], \tag{9}$$

The cross term $-2\rho\, r_1 r_2$ encodes the correlation between observables: for positively correlated data ($\rho > 0$) and residuals with the same sign ($r_1 r_2 > 0$), it reduces the effective penalty in the likelihood, indicating that joint